

Structural determination of symbiotic nodulation factors from the broad host-range *Rhizobium* species NGR234

Neil P.J. Price^{a,1,b,*}, Franck Talmont^a, Jean-Michel Wieruszeski^c,
Danielle Promé^a, Jean-Claude Promé^a

^a Laboratoire de Pharmacologie et de Toxicologie Fondamentale du Centre National de la Recherche Scientifique, 205 Route de Narbonne, 31077 Toulouse, France

^b Laboratoire de Biologie Moléculaire des Plantes Supérieures, Université de Genève, 1 Chemin de l'Impératrice, CH-1292 Chambésy / Geneva, Switzerland

^c Laboratoire de Chimie Biologique et Unité Mixte du CNRS, Université des Sciences et Techniques de Lille Flandres-Artois, Villeneuve d'Ascq, France

Received 9 January 1996; accepted 15 April 1996

Abstract

Nod factors are secreted lipo-oligosaccharides produced by symbiotic nitrogen-fixing *Rhizobium* bacteria that induce nodule formation on the roots of host leguminous plants. Two biologically active fractions (NodNGR_A and NodNGR_B) were isolated by reversed-phase HPLC from the culture supernatant of a Nod factor overproducing strain of *Rhizobium* sp. NGR234. NodNGR_A and NodNGR_B are heterogeneous mixtures of *N*-acylated 2-*O*-methylfucosylated chitomers, in which the fucosyl residue may be either 3-sulfated (NodNGR_A), or 4-*O*-acetylated or nonsubstituted (NodNGR_B). Structurally analogous series of compounds occur with either *N*-vaccenic (C18:1) or *N*-palmitic (C16:0) substituents. The presence of 6-*O*-carbamoyl groups on the GlcNMeAcyl residue occurs on some molecules, while others are di-*O*-carbamoylated.

Abbreviations: FABMS, fast-atom bombardment mass spectroscopy; COSY, correlation spectroscopy; CAD-MIKE, collision activated dissociation-mass analysed ion kinetic energy; DEPT, distortionless enhancement by polarization transfer; TFA, trifluoroacetic acid; TLC, thin-layer chromatography; NMR, nuclear magnetic resonance spectroscopy; HPLC, high-performance liquid chromatography; GLC, gas-liquid chromatography

* Corresponding author. Tel.: +1-315-4706858; Fax: +1-315-4706856.

¹ Current address: Department of Chemistry, SUNY College of Environmental Science and Forestry, Syracuse, NY 13210, USA.

Detailed structural analysis of seventeen Nod factors are reported here. © 1996 Elsevier Science Ltd.

Keywords: Structural determination; *Rhizobium*; Nod factor

1. Introduction

Rhizobium are nitrogen-fixing bacteria that induce root nodules on leguminous plants [1,2]. Rhizobial infection and the ensuing nodule development are host specific in that a particular *Rhizobium* species will only nodulate a limited range of host plants. The ability to form nodules is determined by the rhizobial nodulation (*nod*) genes. Common and regulatory *nod* genes (*nodABC* and *nodD*, respectively) are present in all *Rhizobium* species and are essential for nodule formation, while other, host-specificity *nod* genes determine the symbiotic host range [2]. The initial recognition between potential symbionts is determined by legume derived flavanoids [3] that induce transcription of most of the *nod* genes. In response, *Rhizobium* synthesize and secrete lipo-oligosaccharidic compounds called Nod factors. Nod factors cause the host-specific root-hair deformations normally characteristic of early rhizobial infection, and at higher concentrations Nod factors have also been shown to induce root nodule formation in the absence of *Rhizobium* bacteria [7,10].

Nod factors consist of a common *N*-acylated chitomeric core that may be structurally modified depending upon the rhizobial species [2,5]. *Rhizobium* host specificity and the biological activity of Nod factors is determined by the various substituents to the core structure. Thus *R. meliloti* Nod factors are 6-sulfated on the reducing GlcNAc and C16:2 acylated on the terminal nonreducing sugar [4,5], while *R. leguminosarum* factors are nonsulfated and have a conjugated C18:3 lipid component [6]. Sulfated signals, for example NodRm-IV(Ac, S), induce nodules and root-hair deformations on *Medicago sativa* (alfalfa) [7,8], a host plant of *R. meliloti*, while nonsulfated factors, derived from either *R. leguminosarum* or *nodH*[−] mutant strains of *R. meliloti*, are biologically active upon *Vicia sativa* (common vetch) [6,8], a host plant of *R. leguminosarum*. Nod factors have also been isolated from *Bradyrhizobium japonicum* (NodBj), *Azorhizobium caulinodans* (NodAc), *R. tropici* (NodRt) and *R. fredii* (NodRf) (reviewed in ref. [9]). The *Bradyrhizobium* Nod factors (NodBj) were 6-*O*-glycosylated with 2-*O*-methylfucose or fucose on the reducing sugar and *N*-acylated either with C18:1 or C16:0. Some were acetylated and/or carbamoylated on the terminal nonreducing sugar. Similarly, *Azorhizobium* Nod factors were 6-*O*-glycosylated, but in this case with L-arabinose, and were *N*-acylated with either C18:1 or C18:0. The *N*-acylated sugar of the NodAc factors was also *N*-methylated and 6-*O*-carbamoylated. NodRt factors also consist of a *N*-methylated chitopentaose backbone, some of which may be 6-sulfated on the reducing *N*-acetylglucosamine residue. *R. fredii* Nod factors consist of a series of substituted $\beta(1 \rightarrow 4)$ -linked trimers, tetramers and pentamers of *N*-acetylglucosamine, which were *N*-acylated with vaccenic acid, and 2-*O*-methylfucosylated on C-6 of the reducing residue.

Rhizobium species NGR234 is of primary interest because of its particularly broad

host range, which includes at least 70 genera of legumes [10]. We have previously reported the biological properties of Nod factors from the broad host-range *Rhizobium* sp. NGR234 on a number of legume host species [1]. Here we describe details of the structural characterization of seventeen Nod factors from an apigenin-induced, overproducing strain of NGR234 by a combination of chemical analysis, MS and NMR techniques.

2. Experimental procedures

Materials.—Chemicals were obtained from Aldrich, France, and radiolabelled compounds were from Amersham. Solvents were redistilled. Silica Gel-60 thin-layer plates were from Merck. The Nod factor overproducing strain NGR234(pA28) containing extra copies of the NGR234 *nodD1* gene has been described previously [1].

Identification and isolation of Nod factors.—*Rhizobium* cultures (10 mL) were radiolabelled by the inclusion of 1 μ Ci/mL sodium [35 S]sulfate, sodium [14 C]acetate, or [1- 14 C]glucosamine at the start of the growth period. After 18 h the culture supernatant was passed through a C₁₈ Sep-Pak cartridge (Waters), washed with H₂O (5 mL), and eluted with MeOH (3 mL). Radiolabelled metabolites in the MeOH extract were separated by thin-layer chromatography on Silica Gel-60 plates using 5:4:1 CHCl₃–MeOH–H₂O and detected either by autoradiography, scintillation counting, or with a Berthold linear scanner. Larger volumes (> 10 L) of centrifuged culture supernatant were extracted by passing through a column (20 \times 3 cm) of Lichroprep RP₁₈ (Merck), and after washing with 50 vol water, were eluted under medium pressure with 10 vol of MeOH. The MeOH phase was evaporated under vacuum, redissolved in H₂O, and extracted with EtOAc. The aqueous phase was lyophilised and purified further by reversed-phase HPLC. Radiolabelled Nod factors were used as markers for the isolation procedures.

Chromatography.—The HPLC apparatus consisted of two Waters 510 pumps, a Waters 660 gradient programmer, and a Shimadzu SPD-64 variable wavelength UV detector. Nod factors were separated on a semipreparative C₁₈ reversed-phase Lichrosorb column (7.5 \times 300 mm; 10 μ m particle size) using isocratic conditions of 2:8 acetonitrile–water for 10 min, followed by a linear gradient to 100% acetonitrile at a flow rate of 2 mL/min. Further separation was achieved on an analytical amino-bonded column (Spherisorb NH₂, 250 \times 150 mm, 3 μ m particle size) using a linear gradient from 100% acetonitrile to 100% water at a flow rate of 0.5 mL/min. The eluent was monitored at 206 nm. Gas chromatographic analysis was carried out on a Girdel 30 instrument using a 30 m capillary OV1 column (Spiral, France), a Ross injector, and flame ionisation detector. Helium was used as carrier gas.

Carbohydrate analysis.—Nod factors were hydrolysed with aq TFA (4 M, 4 h, 110 °C). After drying under nitrogen, the residues were reduced overnight with M borohydride or borodeuteride in 100 mM NH₄OH. Peracetylation was performed with 1:1 acetic anhydride–pyridine (overnight, room temperature). Deacetylation was achieved with methanolic sodium methoxide (0.5 M, 40 °C, 1 h). Methyl glycosides were prepared with anhydrous methanolic HCl (M, 1 h, 80 °C). After evaporation of solvent,

Me₃Si derivatives were prepared as described previously [11]. GLC assignments were made by comparison with authenticated standards and by electron-impact mode GLC–MS. Sugars were assigned to the D- or L-series by GLC analysis of their Me₃Si (–)-2-butanoyl glycosides [12].

Lipid analysis.—Lipids were recovered from the TFA hydrosylate (4 M, 4 h, 110 °C) or after saponification (5% aq KOH, 18 h, 80 °C) by extraction into diethyl ether. Methyl esters were prepared with diazomethane. Hydrogenation of double bonds was achieved at atmospheric pressure (1 h, 25 °C) using 10% Pd-on-carbon catalyst in MeOH. Perfluorobenzyl (PFB) derivatives were prepared as described [13] from pentafluorobenzyl bromide catalysed with diisopropylethylamine, and analysed by negative ion mode GLC–MS/MS. The location of the double bond was deduced from carboxylate anions generated by dissociated electron-capture ionisation of the PFB derivatives as analysed by collision activated dissociation-mass analysed ion kinetic energy spectrometry (CAD-MIKES). Dimethyldisulfide (DMS) ether derivatives of methylated fatty acids were prepared as described [14,15] and examined by GLC–MS in the electron-impact mode.

Periodate oxidation and methylation analysis.—Permethylation analysis was performed on borodeuterohydride-reduced compounds according to Parente et al. [16]. Permethylated derivatives were hydrolysed, reduced with borohydride, and peracetylated [16]. The resulting partially methylated alditol acetates were examined by GLC–MS, in both electron-impact and chemical-ionisation modes. Periodate oxidation was done with 500 µg of sample dissolved in 5 mL of 0.1 M NaOAc, 8 mM NaIO₄, pH 5.5, in the dark at 4 °C for 8 days. The reaction was stopped by adding 25 mL of ethylene glycol. The pH was adjusted to 7, and products were reduced with NaBD₄. The reaction products were purified by reversed-phase HPLC as described above and analysed by FABMS.

Mass spectrometry.—Fast-atom bombardment mass spectra were recorded on a VG Analytical ZAB-HS instrument. A mixture of 1:1 *m*-nitrobenzyl alcohol–glycerol was the matrix used in both positive and negative detection modes. An accelerating voltage of 6 keV was used, and a xenon beam energy of 8 keV. FAB tandem mass spectrometry using mass analysed kinetic energy spectra (MIKES) were recorded on the same instrument. The reactant gas for negative chemical ionization was methane, and collision-activated dissociations (CAD) were promoted with helium. Electrospray mass spectra were obtained on a PE Sciex APIII Biomolecular Mass Analyser. Samples (10 µg/mL) were dissolved in 2 mM ammonium formate in formic acid (0.1% in 50% aq acetonitrile) and introduced at a flow rate of 2 mL/min. Capillary GLC–MS was recorded by chemical ionization with ammonia as reactant gas or electron impact in positive-ion detection mode on either ZAB-HS or Hewlett–Packard 5989 instruments.

NMR spectrometry.—Solutions of Nod factors were exchanged several times in deuterated aq MeOH with intermediate lyophilisation. NMR spectra were recorded on a Bruker AM-400 WB spectrometer operating in the Fourier-transform mode at a probe temperature of 300 K. Chemical shifts were measured relative to sodium 4,4'-dimethyl-4-silapentane-1-sulfonate (DSS). The samples were dissolved in deuterated MeOH at a concentration of 2.5 mg/0.5 mL for sulfated NodNGR_A, 0.1 mg/mL for acetylated NodNGR_B, and 14.5 mg/0.5 mL for deacetylated NodNGR_B. Homonuclear and

heteronuclear COSY, and DEPT spectra were recorded using the standard pulse sequences supplied by Bruker.

3. Results

Production of Nod factors.—Production of Nod factors was about 2 mg/L of culture medium. Two fractions, NodNGR_A and NodNGR_B, were separated by reversed-phase HPLC from the overproducing strain NGR234(pA28) [1]. Both fractions could be visualised on TLC plates using orcinol–sulfuric acid reagent. Bacterial feeding experiments with radiolabelled precursors indicated labeling with [1-¹⁴C]acetate, and D-[1-¹⁴C]glucosamine but not with [³²P]phosphate. Fraction NodNGR_A factors were also labelled with [³⁵S]sulfate. Relative elution rates on normal and reverse phase TLC plates and by reversed-phase HPLC suggested that NodNGR_A was more polar than NodNGR_B. UV absorbance maxima were at 206 nm for both fractions, and the absence of phosphate was verified by ³¹P NMR spectrometry. Both fractions were biological activity in root hair deformation (Had) and root hair initiation (Hai) bioassays [1].

Constituent analysis of Nod factors.—After reduction of NodNGR_A and NodNGR_B with NaBD₄ in NH₄OH (0.1 M), the deuterated products were hydrolyzed with trifluoroacetic acid (4 M, 4 h, 100 °C) and extracted with ether. The aqueous phases were evaporated, reduced with sodium borohydride in NH₄OH (0.1 M) and peracetylated. GLC–MS analysis of the corresponding alditol acetates indicated the presence of glucosamine, 2-amino-2-deoxy-*N*-methylhexose and 6-deoxy-2-*O*-methylhexose. Comparison with authentic standards identified these latter sugars as *N*-methylglucosamine and 2-*O*-methylfucose, respectively. The presence of deuterated glucosamine identified this sugar as the reducing residue. Absolute configurations were deduced from the chromatographic behaviour of the (–)-2-butyl glycosides, which indicated D-glucosamine, *N*-methyl-D-glucosamine and 2-*O*-methyl-L-fucose. Released fatty acids from the ether phase were methyl-esterified, and analysis by GLC and GLC–MS indicated approximately 80% C18:1 and 20% C16:0. A dichloromethane extract of the acid-hydrolysed fraction was hydrogenated in the presence of Pd catalyst. The hydrogenated fatty acids were recovered by reversed phase Sep-Pak and converted to their methyl esters. The identification of C18:0 by GLC confirmed that the major lipid present (C18:1) contained a reducible double bond, and the ¹H NMR peaks at 5.34 ppm (Fig. 5) indicating symmetrical or near-symmetrical allylic protons showed that it was nonconjugated.

Further identification of the lipid moieties was demonstrated by collision-induced charge remote fragmentation mass spectrometry of the gas-phase carboxylate anions arising from perfluorobenzyl esters [13]. Low probability of cleavage at double bonds, giving less intense fragmentation ions, allowed the identification of vaccenic acid (C18:1 Δ_{11}) and palmitic acid (C16:0) (Fig. 1A). The vaccenic acid was assigned as *cis* (i.e., 11-*Z*-octadecenoic acid) by GLC comparison with standard compounds, and by ¹³C NMR spectroscopy (see later). Furthermore, the difference in molecular weight between the two lipid groups was consistent with the 26 U differences that were observed in the source FABMS (Fig. 2) and electrospray MS spectra (Table 1).

The *N*-linked C18:1 fatty acid was verified as being vaccenic (C18:1 $\Delta_{11,12}$) rather than oleic acid (C18:1 $\Delta_{9,10}$) from the fragmentation pattern of its methylated DMDS derivative. The fatty acids released by saponification were methylated and reacted with dimethyldisulfide in the presence of iodine [14,15]. The resultant derivatives were examined by GLC–MS. Two GLC peaks were observed, corresponding to methyl palmitate and the DMDS derivative of methyl vaccenate. Mass spectra of the latter (Fig. 1B) showed a m/z 390 molecular ion and two fragment ions (245 and 145 amu) corresponding to cleavage across the site of the original double bond. The additional peak at m/z 213 is attributable to loss of methanol (32 amu) from the m/z 245 methyl ester fragment. Identical fragmentation was seen for a standard of *cis*-vaccenic acid (C18:1 $\Delta_{11,12}$). By comparison, an oleic acid (C18:1 $\Delta_{9,10}$) standard gave the same molecular ion (m/z 390), but the corresponding fragment ions were 219, 171, and 187 (i.e., 219–32), respectively.

Mass spectrometry.—NodNGR_A and NodNGR_B were examined further by fast-atom bombardment mass spectrometry in both positive and/or negative-ion detection modes (Fig. 2). Both fragments gave molecular ion peaks in the 1400–1600 mass range. Spectra of NodNGR_B were obtained with positive-ion detection (Fig. 2A), whereas spectra of NodNGR_A were better in the negative mode (Fig. 2B), consistent with the NodNGR_A Nod factors carrying a negatively charged sulfate group.

Positive-ion FAB mass spectra of NodNGR_B revealed two major peaks (m/z 1558 and 1516) in the high mass region (Fig. 2A), and the 42 U difference between them suggested that the former was a mono-acetylated analog of the latter. Two other peaks, 43 U less at m/z 1515 and 1473, were also separated by 42, indicating that other mono-acetylated Nod factors were also present. These two sets of doublets were separated from each other by 43 U which were tentatively assigned as carbamoyl groups. Two series of fragments arising from cleavage of glycosidic bonds were clear. Ions at m/z 1135 and 1092, arising after loss of the reducing terminus, fragmented further by three sequential losses of *N*-acetylglucosamine residues (each 203 U) to give stable m/z 526 and 483 ions. These were attributed to the terminal nonreducing residues. In positive-ion mode, these fragmentations are due to the formation of oxonium ions at each glucosaminyl linkage with charge retention on the nonreducing part (B ions) [17]. The retention of the 43 U difference throughout these fragmentations indicated that the carbamoyl groups were located on the terminal nonreducing sugars. A more minor fragment ion at m/z 440 was assigned as arising from a non-carbamoylated Nod factor (molecular ion at $[M + H]^+ = 1430$). Its observed mass corresponded to that for *N*-methylglucosamine, *N*-acylated with vaccenic acid, and suggested that the *N*-acyl and *N*-methyl groups were also attached to the terminal nonreducing sugar.

Fig. 1. Identification of the *N*-linked lipid chains from *Rhizobium* sp. NGR234 Nod factors. (A) Lipids were hydrolysed, perfluorobenzylated, and separated by GLC on OV1. Tandem MS/MS spectra (MIKES) were recorded of the carboxylate anions generated by dissociative electron capture. Top: palmitate (C16:0); bottom: *cis*-vaccenate (11-*Z*-C18:1). (B) E.I. mass spectra of DMDS-methyl vaccenate. Base hydrolyzed fatty acids were treated with methanolic BF₃ and derivatized across double bonds with dimethyldisulfide (DMDS) in the presence of iodine [14,15]. GLC–MS (E.I. mode) fragmentations localized the double bond as Δ_{11} , indicating vaccenic acid (C18:1 Δ_{11}).

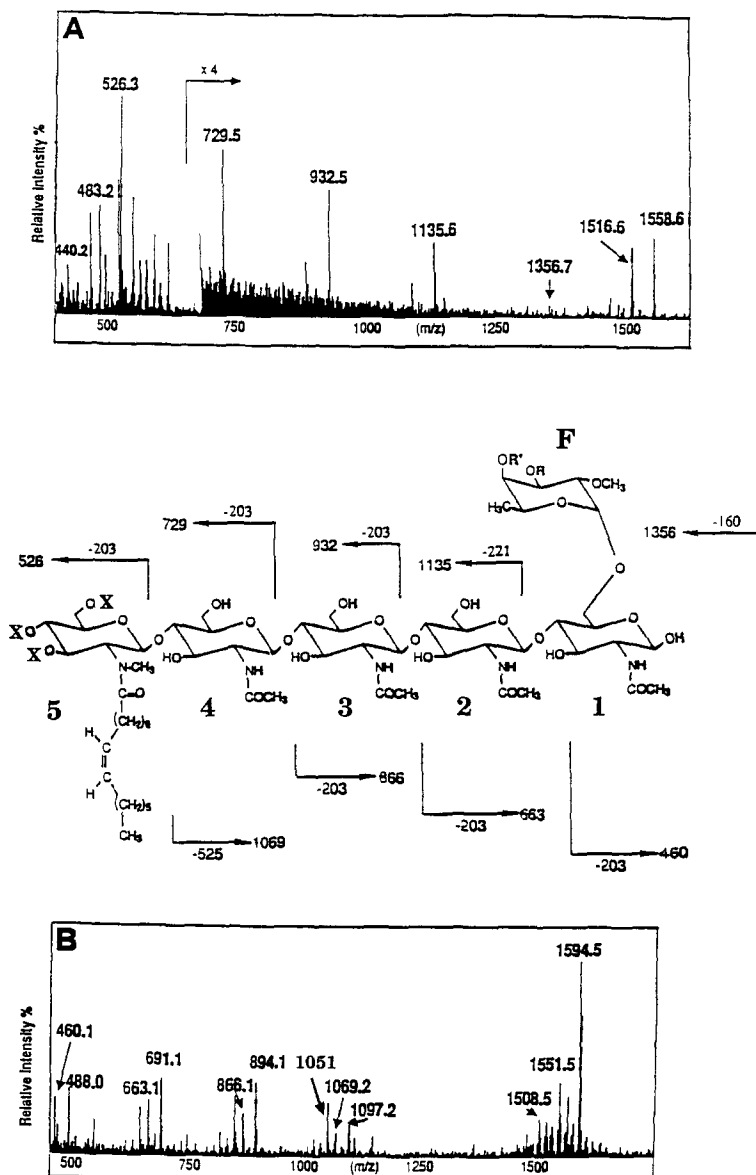


Fig. 2. Fast bombardment mass spectrometry. (A) Positive-ion detection mode of NodNGR_B (R = H, R' = acetate). (B) Negative-ion detection mode of NodNGR_A (R = SO₃H, R' = H). Core fragmentation assignments are shown. X = H or carbamoyl (0, 1 or 2).

In the negative-ion detection mode, NodNGR_A gave prominent $[M - H]^-$ ions (Fig. 2B). The major of these, at m/z 1594 and 1551, differed by 43 U and were assigned as mono- and dicarbamoylated species, *N*-substituted with vaccenic acid. Weaker $[M - H]^-$

Table 1

Electrospray mass spectrometry of sulfated NodNGR_A Nod factors ^a

<i>Rhizobium</i> sp. NGR234 Nod factor ^b	Observed mass ions		
	[M + Na ₂] ⁺	[M + Na + NH ₄] ⁺	<i>M_t</i> ^c
NodNGR-V(Cb ₂ , NMe, C18:1)(MeFuc, S)	1641	1636	1595
NodNGR-V(Cb ₂ , NMe, C16:0)(MeFuc, S)	1615	1610	1569
NodNGR-V(Cb ₁ , NMe, C18:1)(MeFuc, S)	1598	1593	1552
NodNGR-V(Cb ₂ , NMe, C16:0)(MeFuc, S)	1572	1567	1526
NodNGR-V(NMe, C18:1)(MeFuc, S)	1555	1550	1509
NodNGR-V(NMe, C16:0)(MeFuc, S)	n.d. ^d	n.d.	1483

^a Positive-ion mode detection spectra were obtained on NodNGR_A in ammonium formate (2 mM)–formic acid (0.1%) buffer in 50% aq acetonitrile.

^b Nomenclature as described in ref. [8].

^c Calculated molecular mass.

^d Not detected.

ions were also observed 26 U less, at m/z 1568 and 1525, which were again separated by 43 U. The 26 U differences suggested groups of Nod factors differing by an ethylidene (–CH=CH–) moiety, corresponding to the difference between vaccenic (C18:1) and palmitic (C16:0) acids. The 43 U differences were again attributable to carbamoyl groups. An additional minor peak at m/z 1508 was due to *N*-vaccenated Nod factor without any carbamoyl substituents. Fragmentations of the [M – H][–] from fraction A are relatively more complex since 1.5X, Y and Z ions [17] are generated at each glucosaminyl bond.

In positive-ion mode spectra of NodNGR_A the expected [M + H]⁺ molecular ions were weak (data not shown), but an intense [M – SO₃]⁺ ion resulting from the loss of 80 U was observed at m/z 1516. The inclusion of KI or NaI in the matrix increased this mass to m/z 1672 [M + 2K – H]⁺, 1656 [M + K + Na – H]⁺, or 1640 [M + 2Na – H]⁺, respectively. Similar adduct ions were also observed 43 U less although at lower intensity because of the lesser amounts present. Characteristic losses of 118 or 102 U due to [KSO₃] or [NaSO₃] confirmed that only one sulfate group was present.

The presence of carbamoyl substituents on the terminal nonreducing glucosamine was verified by deuterioacetylation of the free OH groups on the Nod factors. This increased the observed masses of the terminal nonreducing fragments (m/z 440, 483, and 526; see Fig. 2A) by 135, 90, and 45 U, respectively, indicating a mixture of compounds bearing either none, one, or two carbamoyl moieties on the nonreducing end. These data, which were obtained on both NodNGR_A and NodNGR_B, were corroborated by characteristic carbonyl resonances in the ¹³C NMR spectrum (Fig. 7).

FAB mass spectra of NodNGR_B were also obtained after reduction with NaBD₄ to deuterium-label the reducing sugar. Three parallel sets of fragmentations differing by 43 U were observed (Fig. 3). The reductive deuteration removed the *O*-acetyl group, and increased the m/z 1356, 1313, and 1270 fragments by 3 U to 1359, 1316 and 1273, respectively, indicating that the reducing sugar was GlcNAc with the 2-*O*-MeFuc as a branched side chain. Sequential fragmentations occurred by loss of 160, 223, 203, 203, 203 U for all three compounds giving rise to stable fragments at m/z 526, 483, and 440.

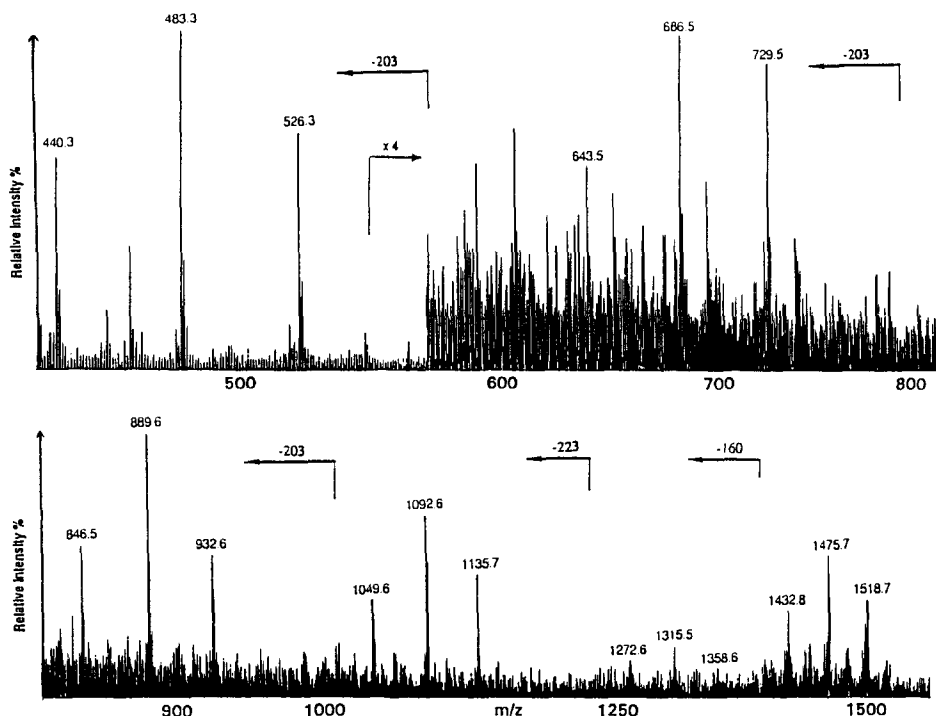


Fig. 3. FAB/MS spectrum of NodNGR_B after *O*-deacetylation and reduction with sodium borodeuteride. Losses are 160 (2-*O*-MeFuc), 223 (reducing GlcNAc), 203 (GlcNAc-2), 203 (GlcNAc-3), 203 (GlcNAc-4). The triplets of peaks throughout the spectrum arise from di- (m/z 1518.7), mono- (m/z 1475.7), and noncarbamoylated (m/z 1432.8) Nod factors.

Losses of 223, 203, and 160 U correspond, respectively, to the deuterated GlcNAc reducing sugar, sequential GlcNAc oxonium ions, and cleavage of the 2-*O*-MeFuc residue. The 43 U differences were still seen after reduction but relative intensities had changed, suggesting that the carbamoyl groups were only partially stable to borodeuteride reduction, with the major dicarbamoyl compound being partly degraded to mono- and non-carbamoylated Nod factors. The retention of the 43 U differences throughout the fragmentations confirmed that the carbamoyl groups were located on the nonreducing sugar.

Mass spectra of component Nod factors were obtained by tandem MS/MS [10]. Fragmentations arising from selected high mass molecular ions were observed by MIKE spectrometry (Fig. 4). Pseudomolecular $[M + H]^+$ ions due to acetylated NodNGR_B factors (m/z 1558 and 1515, Fig. 4B and Fig. 4A, respectively) fragmented by loss of an acetylated 2-*O*-methylfucosyl-GlcNAc moiety (423 U) from the reducing terminus. Furthermore, the loss of 60 U from m/z 1558 (Fig. 4B) is attributable to the acetate group. The corresponding non-acetylated NodNGR_B species (m/z 1516) (Fig. 4A) lost 381 U from the reducing end due to a non-acetylated 2-*O*-MeFuc-GlcNAc disaccharide group, clearly indicating that the *O*-acetyl group was attached to the reducing end of the molecule.

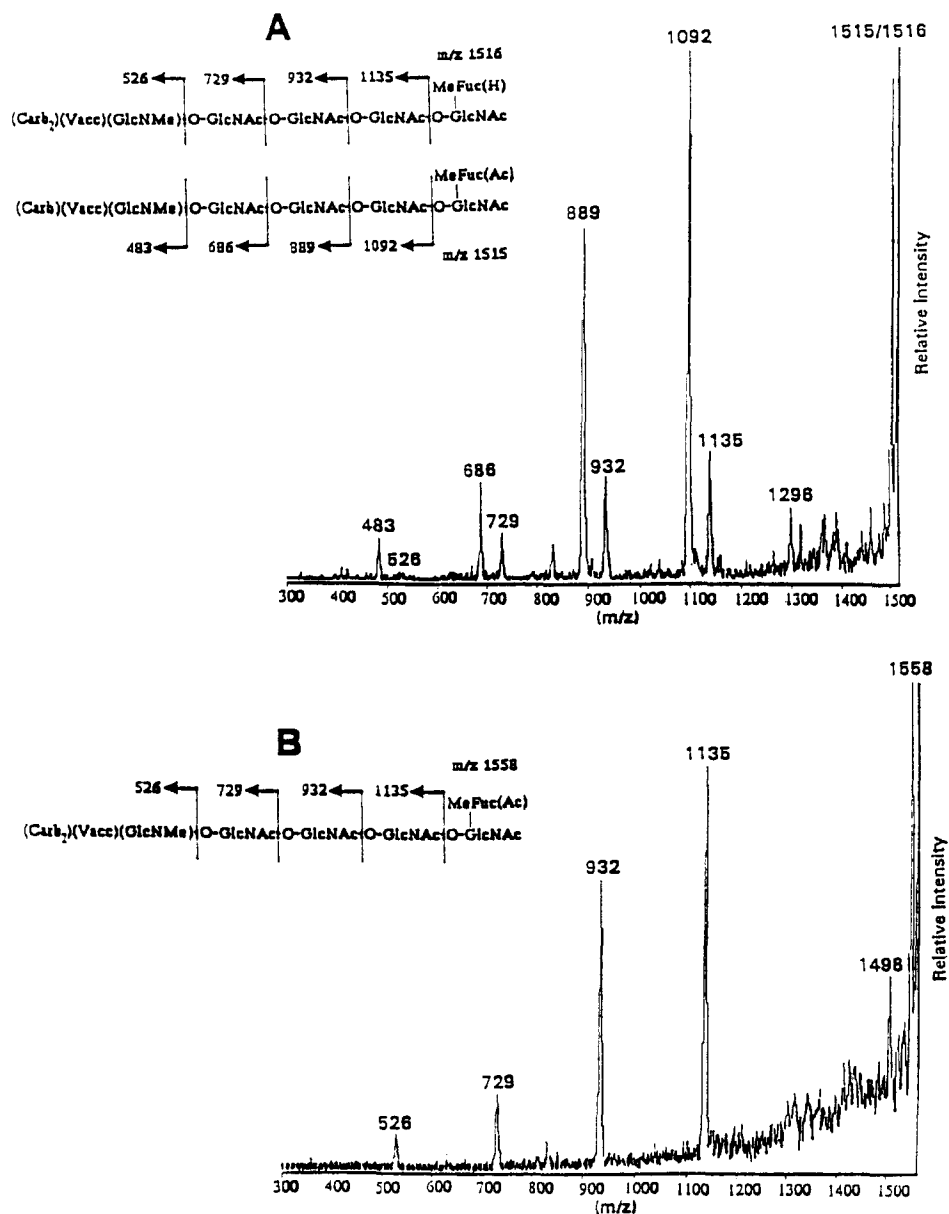


Fig. 4. FAB/MS: mass ion kinetic energy spectra (MIKES) of NodNGR_B. (A) 4-*O*-acetylated mono-carbamoylated NodNGR_B (m/z 1515) and nonacetylated dicarbamoylated NodNGR_B (m/z 1516); (B) 4-*O*-acetylated dicarbamoylated NodNGR_B (m/z 1558). Assignments as are shown.

Electrospray mass spectrometry of the sulfated Nod factor revealed a series of $[M + Na_2]^+$ and $[M + Na + NH_4]^+$ pseudomolecular ion peaks (Table 1). The two most intense m/z 1641 and m/z 1636 were assigned to the dicarbamoylated and

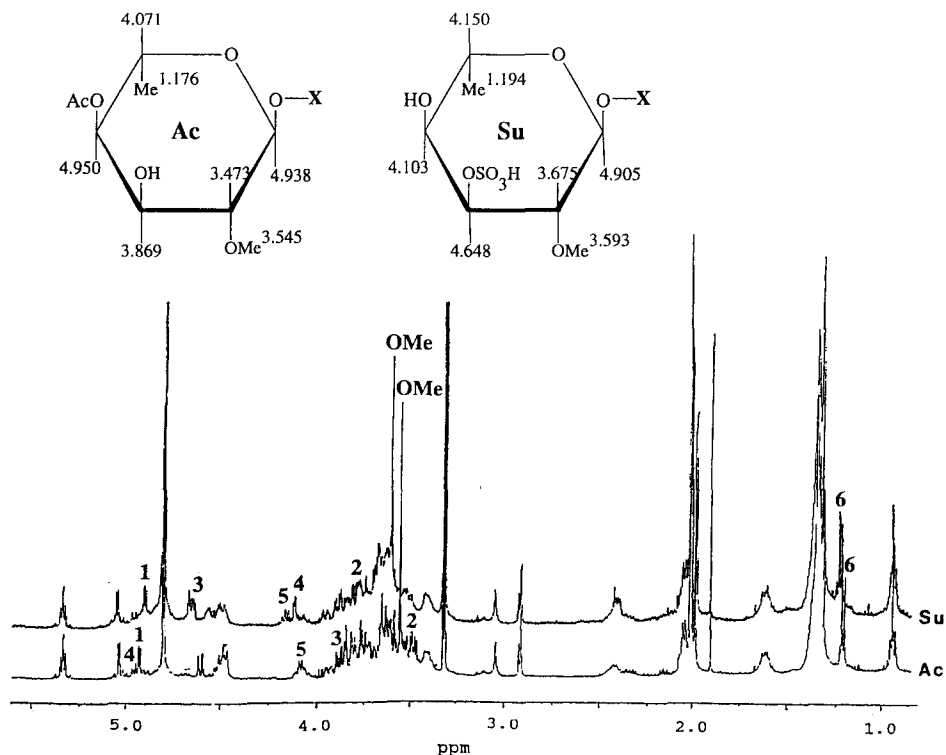
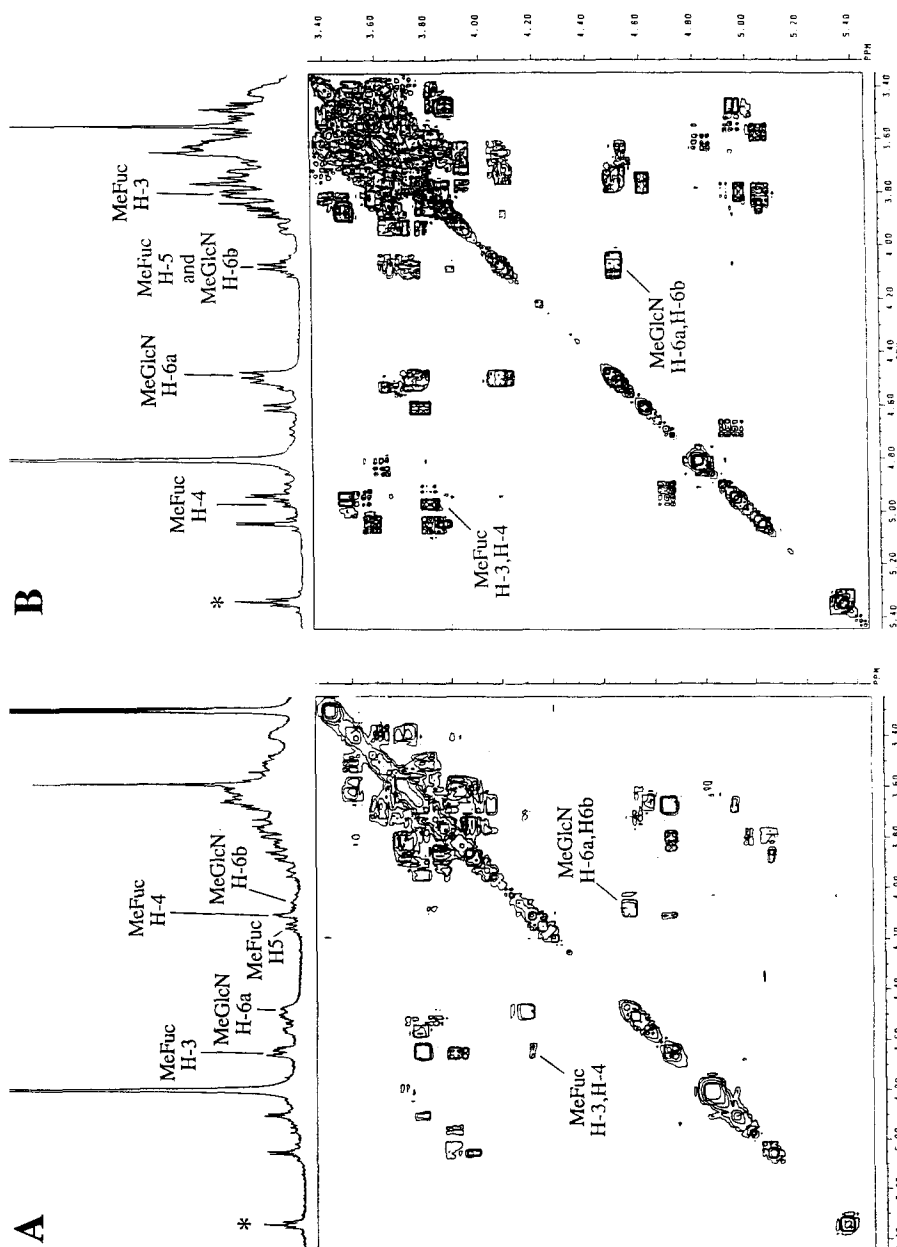
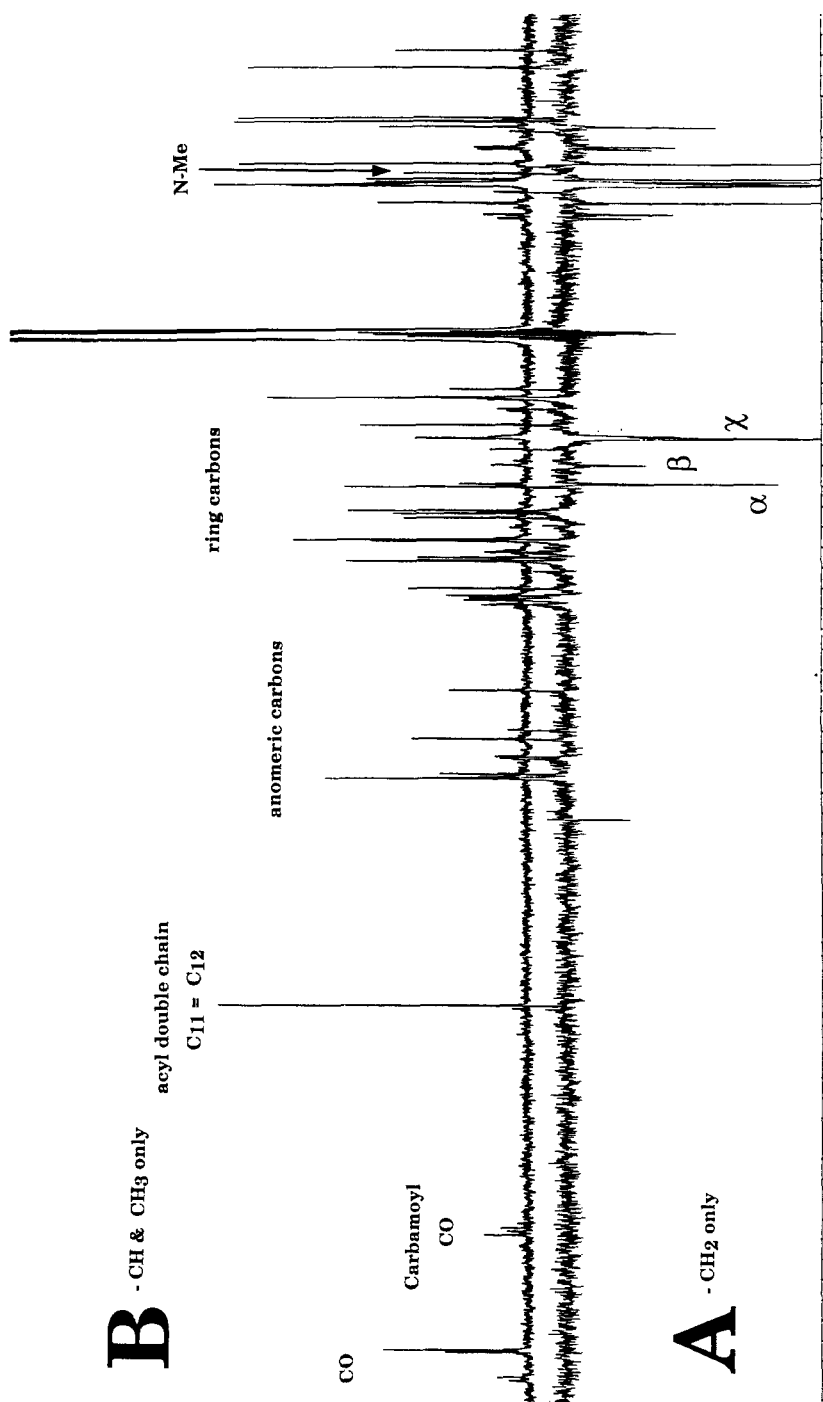


Fig. 5. Overlay plot of the ¹H NMR spectra of 3-sulfated NodNGR_A (Su) and 4-O-acetylated NodNGR_B (Ac). Differences in chemical shifts (assigned 1 to 6 and OMe) are confined to the 2-O-methylfucosyl residues, as shown in the detail. Ac, acetyl; Me, methyl; X, glycosidic linkage.

N-vaccenoylated Nod factor. Peaks due to $[M + (NH_4)_2]^+$ (m/z 1631), $[M + NH_4 + K]^+$ (m/z 1652), and $[M + Na + K]^+$ (m/z 1657) ions were also observed for this compound. No fragmentation occurred, but doubly charged Na adduct ions arising from the major molecular species were observed at m/z 832 and m/z 827. Other peaks were seen 43 (carbamoyl group) and 26 ($-\text{CH}=\text{CH}-$ group) U less than the most intense peaks, confirming the FAB/MS observations. Interestingly, peaks due to the dicarbamoylated *N*-palmitoylated Nod factor were more intense than those from the monocarbamoylated *N*-vaccenoylated species. Assuming equivalent detector response, this suggested that the dicarbamoylated *N*-palmitoylated Nod factor is the second most abundant component in the sulfated fraction, and is more prevalent than the mono-carbamoylated *N*-vaccenoylated compound. Furthermore, no molecular ion was seen for the noncarbamoylated NodNGR-V(NMe, C16:0)(MeFuc, S) Nod factor, indicating that this compound is either not produced or is present at very low concentration.

Fig. 6. Homonuclear ¹H-¹H COSY spectra of (A) 3-sulfated NodNGR_A, and (B) 4-O-acetylated NodNGR_B. MeFuc, 2-O-methylfucosyl; MeGlcN, *N*-acetyl-*N*-methyl-glucosaminy; *, allylic protons.





Permethylation and periodate oxidation.—Permethylation of NodNGR_A and NodNGR_B by the Paz Parente procedure [16] confirmed the (1 → 4)-linkages between glucosamines and the (1 → 6)-attachment of the 2-*O*-methylfucose, the presence of *N*-methylglucosamine, and the location of the 2-*O*-methyl group on the fucosyl residue. Furthermore, permethylation of NodNGR_B gave rise to a 2,3,4-tri-*O*-methylated fucose derivative, whereas the equivalent residue on NodNGR_A compounds gave 2,4-di-*O*-methylated fucose. This was because the sulfate group was stable during the permethylation procedure, effectively blocking the 3-*O* position from methylation and, therefore, demonstrated that the sulfate group occupied the fucosyl 3-*O* position. However, the carbamoyl groups, and the NodNGR_B *O*-acetyl moiety were labile in the strongly basic conditions used for methylation, and their location could not be confirmed by this technique. Periodate oxidation of NodNGR_A or NodNGR_B was not possible, indicating that O-3 or O-4 of the terminal nonreducing sugars were substituted, presumably by at least one carbamoyl residue.

NMR spectroscopy.—The spectra of NodNGR_A and NodNGR_B were plotted in overlay to highlight dissimilarities (Fig. 5). Major differences were confined to the 2-*O*-Me-fucosyl protons, confirming that structural differences between the Nod factors are located on this residue. Analysis of the ¹H NMR (Fig. 5) and 2D homonuclear COSY (Fig. 6) spectra of NodNGR_A and NodNGR_B, and the DEPT (Fig. 7) and ¹³C-¹H Correlation spectra (Fig. 8) of *O*-deacetylated NodNGR_B made possible the complete assignment of the 2-*O*-methylfucosyl protons (Table 2). In all spectra anomeric proton signals were present for GlcNAc reducing sugars, α-(2-*O*-methylfucose, βGlcNMe(Acyl), and for βGlcNAc residues. The presence of the GlcNAc residues was confirmed by the *N*-acetyl methyl signals (1.9–2.0 ppm), and by the GlcNAc H-1 and H-6 reporter group protons [18]. Signals due to H-1α of the reducing GlcNAc were evident at δ 5.044 (acetylated) and δ 5.054 (sulfated). The 4-*O*-acetyl group on NodNGR_B was relatively unstable with time, leading to a predominantly *O*-deacetylated fraction. Signals due to H-6 of the reducing GlcNAc were evident at δ 3.945 (NodNGR_A) and δ 3.743 (NodNGR_B), shifted +0.07 and +0.093 ppm, respectively, by 6-*O*-(2-*O*-Me)fucosylation. These values compare favourably with the +0.105 ppm chemical shift difference observed for 6-*O*-fucosylation of the terminal GlcNAc of N-linked glycoproteins [18].

NodNGR_B gave two doublet in the 5 ppm region due to anomeric proton resonances. The resonance at δ 5.043 (*J*_{1,2} = 3.19 Hz) was assigned to H-1α of the reducing sugar [4,6], and the signal at 4.937 (*J*_{1,2} = 3.51 Hz) is evidence for the H-1α of 2-*O*-methylfucose (δ 4.90 for H-1α of fucose linked to position-6 of a reducing *N*-acetylglucosamine from *N*-glycan [18]). These values were confirmed by heteronuclear ¹H-¹³C

Fig. 7. Proton-decoupled DEPT (A) and ¹³C NMR (B) spectra of NodNGR_B. Carbonyl resonances at 159 to 162 ppm are characteristic of carbamoyl esters. Anomeric (C-1) carbon signals are indicative of β-(1 → 4)-linked D-GlcNAc (104.11 ppm), β-(1 → 4)-linked D-GlcNMeAcyl (103.54 ppm), and α-(1 → 6)-linked 2-*O*-methyl-L-fucose (99.73 ppm). Anomeric forms of GlcNAc-1 are assigned at 92.91 ppm (α-anomer) and 97.37 ppm (β-anomer). The acyl double bond is evident from the overlapping peaks at 132 ppm. DEPT negative signals due to methine C-6 carbons are labeled for 6-*O*-(2-*O*-Me)fucosylated GlcNAc-1 (α), 6-*O*-carbamoylated GlcNMe(acyl) (β), and GlcNAc-2,3,4 (χ) as indicated.

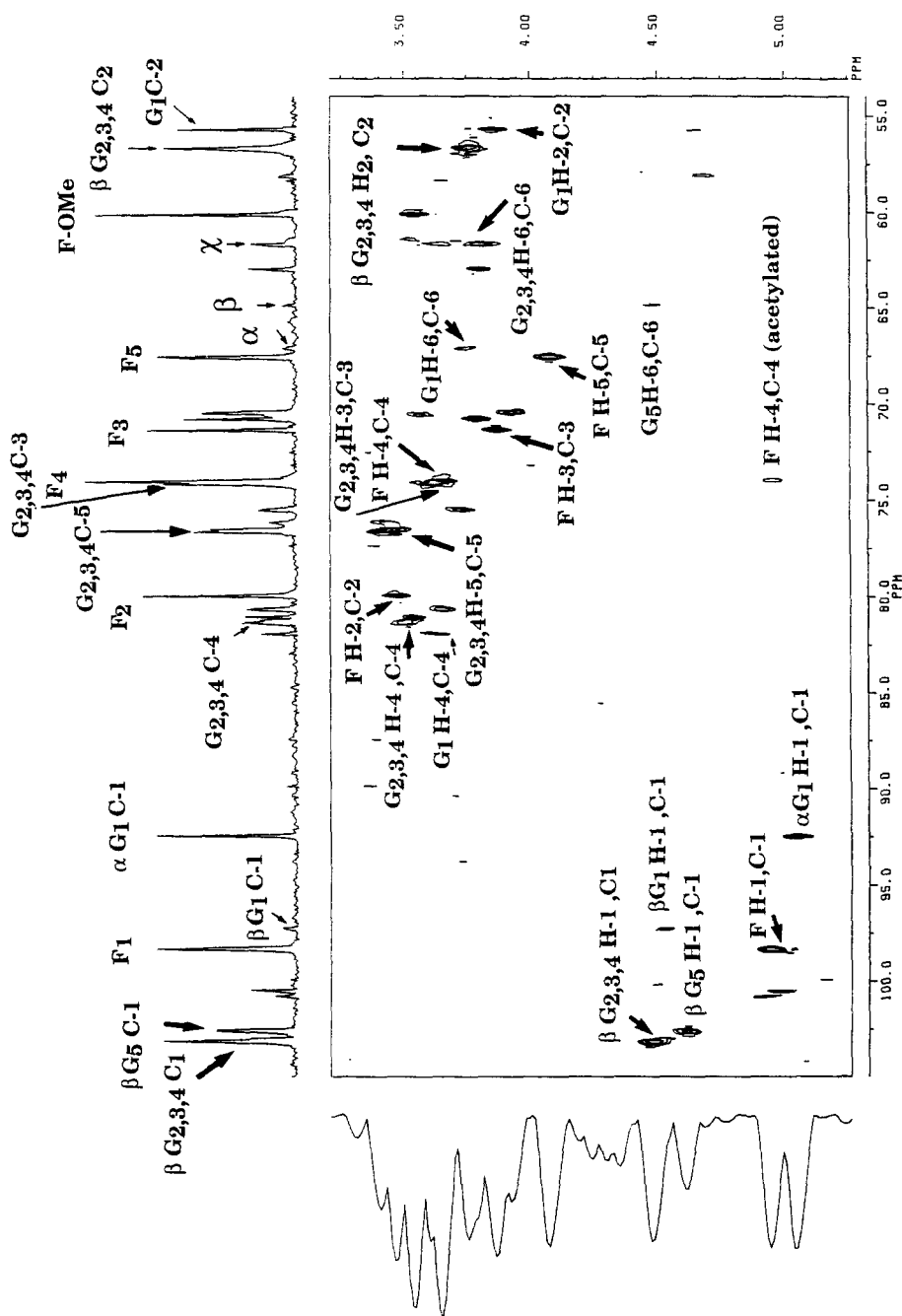


Fig. 8. Heteronuclear ^1H - ^{13}C COSY spectrum of NodNGR₃. Methine C-6 carbons (α , β and χ) were assigned from the DEPT spectrum (Fig. 7). D-GlcNAc-2,3,4 methine C-6 signals (χ , 61.648 ppm) each correlate to two protons, H-6a (3.801 ppm) and H-6b (3.637 ppm). The analogous 6-*O*-carbamoylated C-6 of the GlcNMe(acyl) residue (β , 64.921 ppm) correlates to the corresponding H-6a (4.481 ppm) and, likewise, 6-*O*-(2-*O*-Me)fucoylated C-6 of GlcNAc-1 (α , 67.189 ppm) correlates to H-6a (3.743 ppm). F, 2-*O*-methylfucoyl; G, *N*-acetylglucosaminyl.

Table 2

¹H NMR shifts of structural reporter groups of constitutive monosaccharides for the HPLC fractionated Nod factors from *Rhizobium* NGR234

	Reporter group	Chemical shifts ^a	
		NodNGR _A	NodNGR _B
β GlcNAc-1	α H-1	5.054	5.044
	β H-1	4.656	4.528
	H-6a(<i>O</i> -MeOFuc)	3.945	3.743
	NAc	1.988	1.974
β GlcNAc-2	β H-1	4.488	4.695
	H-2	n.d.	3.848
	H-6a	3.875	3.801
	H-6b	n.d.	3.637
	NAc	1.998	1.997
β GlcNAc-3,4	β H-1	4.488	4.480
	H-6a	3.875	3.801
	H-6b	n.d.	3.637
	NAc	1.998	1.997
2- <i>O</i> -MeFuc	α H-1	4.905	4.938
	H-2	3.675	3.473
	H-3	4.648	3.869
	H-4	4.103	4.950
	H-5	4.150	4.071
	6-Me	1.194	1.177
	2- <i>O</i> -Me	3.593	3.545
GlcNMeAcyl	β H-1	4.564	4.520
	H-6a(<i>O</i> -carbamoyl)	4.481	4.481
	H-6b(<i>O</i> -carbamoyl)	4.050	4.050
	NMe	2.913	2.915
<i>N</i> -Vaccenate	–CH=CH–	5.343	5.344
	NR ₂ COCH ₂ –	2.030	2.032
	CH ₂ 's	1.316	1.317
	CH ₃	0.909	0.896

^a Chemical shifts are in ppm relative to internal DSS in CD₃OD.

COSY (Fig. 8). The characteristic H-5 quartet ($J_{5,6} = 6.55$ Hz) is a useful reporter group of glycosidic linkage [18], and for α -(1 \rightarrow 6)-linked fucosyl residues give a reported signal at δ 4.121 [19]. This correlates well with the NodNGR_A and NodNGR_B H-5 signals assigned at δ 4.150 and δ 4.071, respectively. Homonuclear ¹H COSY spectra confirmed these assignments, showing both H-5 signals were clearly coupled to upfield fucosyl H-6 methyl protons at δ 1.194 and δ 1.177, respectively.

The H-3 chemical shift for fucose α -(1 \rightarrow 6)-linked to β GlcNAc has been reported as δ 3.889 ($J_{3,4} = 3.4$ Hz) [18], which correlates with the δ 3.869 assignment for the

Table 3

¹³C NMR chemical shift assignments for the NodNGR_B Nod factors from *Rhizobium* sp. NGR234

Residue		¹³ C NMR chemical shifts	
		NodNGR _B	Lit. values ^a
αC-1	D-GlcNAc-1	92.432	93.1
βC-1	D-GlcNAc-1	97.255	97.8
βC-1(1,4)	D-GlcNAc-2	102.965	104.11
βC-1(1,4)	D-GlcNAc-3,4	103.125	104.11
βC-1(1,4)	D-GlcNMeAcyl	102.614	n.r. ^b
αC-1(1,6)	L-2-OMeFuc	98.352 ^c	101.82
C-2	GlcNAc-1	55.695	56.51
	2-OMeFuc	79.941	70.93
	GlcNAc-2	55.695	57.92
	GlcNAc-3,4	56.706	57.92
	GlcNMeAcyl	60.752	61.7
C-3	GlcNAc-1	n.r.	72.11
	2-OMeFuc	71.355	72.25
	GlcNAc-2,3,4	74.881	74.93
	GlcNMeAcyl	n.r.	76.31
C-4	GlcNAc-1	81.931	82.53
	2-OMeFuc	74.004	74.54
	(1,4)-GlcNAc-2,3,4	81.931	81.82
	GlcNMeAcyl	n.r.	72.59 ^d
C-5	GlcNAc-1	n.r.	79.48
	2-OMeFuc	67.542	69.44
	GlcNAc-2,3,4	77.031	77.40
	GlcNMeAcyl	n.r.	78.78
C-6	GlcNAc-1	67.189 ^e	69.93
	2-OMeFuc	16.562	18.00
	GlcNAc-2,3,4	61.648	62.81
	GlcNMeAcyl	64.921 ^f	62.81
NCOCH ₃	GlcNAc-1	176.377	177.45
	GlcNAc-2,3,4	176.747	177.45
NCOCH ₃	GlcNAc-1	24.819	24.75
	GlcNAc-2,3,4	25.058	24.98
Carbamoyls	GlcNMeAcyl	161.123	
		160.689	160.289 ^g
		159.864	156.0
OCH ₃	2-OMeFuc	60.034	59.0
NCH ₃	GlcNMeAcyl	29.368	31–39
NCOAcyl	N-Vaccenate	178.902	n.r.
C-2	N-Vaccenate	34.223	34.2
C-11=C-12	N-Vaccenate	132.282/132.056	133.0

Table 3 (continued)

	Residue	¹³ C NMR chemical shifts	
		NodNGR _B	Lit. values ^a
C-18 CH ₃	<i>N</i> -vacenate	16.415	14.0
C-17	<i>N</i> -Vacenate	25.058	25.0
C-10, C-13	<i>N</i> -Vacenate	27.611	27.6

^a Cited in the text.^b n.r. = not resolved.^c Reported for nonmethylated α -(1 → 6)-L-fucose.^d Free C-4 on the terminal non-reducing sugar.^e 2-*O*-methylfucosylated C-6 deshielded by 5.581 ppm.^f Carbamoylated C-6 deshielded by 3.273 ppm.^g Carbamoylated C-4 as reported for the antibiotic streptothricin F.

2-*O*-MeFuc H-3 of NodNGR_B. The equivalent signal in sulfated NodNGR_A is shifted downfield +0.759 ppm by the presence of the 3-SO₄ group, and appears at δ 4.648 where it overlaps signals due to the β (1 → 4)-GlcNAc β H-1 proton. This H-3 assignment was made from the COSY spectrum of NodNGR_A that indicated coupling between this signal and that due to the 2-*O*-methylfucosyl H-4 (δ 4.103), and its downfield shift [21] confirmed the location of the sulfate group. β -(1 → 6)-linked fucose H-4 is generally evident as a doublet ($J_{4,5}$ = 0.6 Hz) with a reported chemical shift of δ 3.84 [18,20]. For NodNGR_A this is shifted downfield by the adjacent 3-sulfate to δ 4.103, where it overlaps the multiplet attributed to H-5 (Fig. 5). The 4-*O*-acetylated NodNGR_B H-4 signal is shift downfield, to δ 4.950, as assigned from the COSY correlation to H-3 (δ 3.869). This large shift (+1.11 ppm) agrees with the reported H-4 value for 4-*O*-acetyl-2-*O*-methyl- α Fuc *p* [27] and confirms that the *O*-acetyl substituent is located on position-4 of the methylfucosyl residue.

Heteronuclear COSY showed that the NodNGR_B GlcNAc-1 H-6 (δ 3.743 ppm) correlates to the GlcNAc-1 C-6 signal at 67.189 ppm (Fig. 8). The DEPT negative peak (Fig. 7) confirmed that this was due to a methylene (CH₂) carbon. The two other methylene carbon signals in the glycosidic region of the DEPT spectrum are attributable to the unsubstituted C-6's of GlcNAc-2,3,4 (δ 61.648), and to C-6 of the 6-*O*-carbamoylated GlcNMeAcyl residue (δ 64.921). The GlcNAc-2,3,4 C-6 signal (δ 61.648) was about three times more intense than the other two C-6 peaks due to the GlcNAc-2,3,4 peak overlap, and are coupled to two protons, H-6a and H-6b, at δ 3.801 and δ 3.637. Similarly, the C-6 carbon of GlcNAc-1 is coupled to its H-6a proton at δ 3.743. The 6-*O*-carbamoylated GlcNMeAcyl H-6b resonance (δ 4.050) of NodNGR_B overlapped the 2-*O*-Mefucosyl H-5 signal (δ 4.071), but a strong COSY cross-peak (J > 12 Hz) was seen from here to 4.481 ppm due to geminal coupling to GlcNMeAcyl proton H-6a. Similar H-6a–H-6b geminal coupling of the 6-*O*-carbamoylated residue was seen from

the COSY cross-peak of the sulfated NodNGR_A factors (Fig. 6). Taken together, these data indicate that for both the sulfated and acetylated NodNGR factors one of the carbamoyl groups is 6-*O*-linked to the terminal GlcNMeAcyl residue.

Three ¹³C NMR peaks occur in the region 159–162 ppm (Fig. 7), which in the absence of aromatic carbons is indicative of carbamoyl carbonyls [23,25]. Two arise from the major dicarbamoylated molecule. The other is probably due to the mono-carbamoylated species which was present as a more minor component. Carbamoylation of sugars generally shifts α -carbon signals downfield by 1.9–5 ppm and β -carbons upfield by 0.3–2.7 ppm [25]. The observed shift of the NodNGR_B 6-*O*-carbamoylated GlcNMeAcyl C-6 (δ 64.921) relative to the unsubstituted GlcNAc-2,3,4 C-6 signal (δ 61.648) is +3.273 ppm. By comparison, the reported carbamoylated α -carbon shifts for streptothricin F were 71.5 ppm (carbamoylated) and 68.2 ppm (decarbamoylated), a difference of 3.3 ppm [23].

Further ¹³C NMR assignments are presented in Table 3. Anomeric C-1 resonances in the region 90–105 ppm were assigned to the five carbohydrate types previously determined: β (1 \rightarrow 4)-linked D-GlcNMeAcyl; β (1 \rightarrow 4)-linked D-GlcNAc; α (1 \rightarrow 6)-linked L-2-*O*-MeFuc; and the α - and β -anomers of the D-GlcNAc reducing sugar. Except for the highly deshielded fucosyl C-6 methyl group, all other oligosaccharidic carbons resonated at 55–85 ppm. Signals due to the GlcNAc residues were readily identified as broadened peaks due to their multiplicity and were assigned by reference to previous work on oligochitomers [22]. C-2 on the terminal acylated sugar was deshielded +3.136 ppm by the effect of the adjacent *N*-methyl group [23,26]. The β (1 \rightarrow 4)-linkage between the aminosugars was confirmed by the downfield shifted C-4 signals (δ 81.931). DEPT and ¹³C NMR spectrometry verified the assignment of the C-6 methylene carbons on the amino sugar residues, and confirmed the α -(1 \rightarrow 6)-glycosidic linkage to the 2-*O*-MeFuc residue (Fig. 8). The 2-*O*-methylfucosylated C-6 methylene shift was deshielded by 6.67 ppm, compared to a reported value of 6.7 ppm [18].

¹³C NMR signals due to the α -(1 \rightarrow 6)-linked 2-*O*-MeFuc residue were assigned by reference to data obtained on fucosylated glycopeptides [18,19]. *O*-Methylation of the fucosyl C-2 was apparent from the observed δ 80.101 chemical shift: 9.07 ppm downfield of the reported shift for an equivalent nonsubstituted fucosyl residue [18]. The expected shift due to *O*-alkylation is generally +5–10 ppm, and thus confirming the location of the 2-*O*-methyl group. ¹³C NMR peaks in the low-field region of the spectra in an approximate ratio 3:1 were assigned to the *N*-acetyl and *N*-MeAcyl carbonyls, respectively. Corresponding N-COCH₃ methyl signals were observed at approximately 25 ppm. The reducing GlcNAc N-COCH₃ methyl signal was shifted 0.37 ppm, as observed previously [24].

NMR signals due to the vaccenic acid moiety were also evident. Overlapping triplets at δ 5.343 and δ 5.344 indicated equivalent methine protons, confirming the presence of a nonconjugated double bond. Homonuclear COSY confirmed that these signals were coupled to the adjacent H-10', H-13' protons at δ 2.03, which showed a further correlation to the acyl chain methylene protons (δ 1.316), and successively to the terminal methyl protons (δ 0.90 and δ 0.91) [4]. ¹³C NMR peaks assigned to C-11' and C-12' confirm the presence of a single, nonconjugated double bond [4], and the C-10', C-13' shifts verify that this was in the *Z*-configuration [6].

4. Discussion

The structures of two groups of biologically active Nod factors, designated NodNGR_A and NodNGR_B, from the broad host range *Rhizobium* sp. NGR234, have been elucidated using chemical analysis, mass spectroscopy, and NMR techniques. Composition and configuration of the sugar residues, sequence, and glycosidic linkage sites were investigated, and showed that a core lipo-oligosaccharidic structure D-GlcNMeAcyl- β -(1 \rightarrow 4)-D-GlcNAc- β -(1 \rightarrow 4)-D-GlcNAc- β -(1 \rightarrow 4)-D-GlcNAc- β -(1 \rightarrow 4)-[α -(1 \rightarrow 6)-L-2MeFuc]-D-GlcNAc was common to all the compounds described. Variation in the acyl moiety *N*-linked to the terminal nonreducing sugar was demonstrated, and both *N*-vacenoylated (C18:1) and *N*-palmitoylated (C16:0) Nod factors occur.

The reversed-phase C₁₈ HPLC chromatographic strategy effectively separated NodNGR_A and NodNGR_B. However, FABMS showed that both groups were chromatographically homogenous mixtures of compounds differing by 43 U. FABMS and NMR indicated that the 43 U moieties were carbamoyl groups, *O*-linked to the *N*-acylated, terminal nonreducing sugar. Dicarbamoylated Nod factors predominated, although mono-*O*-carbamoylated, and noncarbamoylated species were also present. DEPT NMR demonstrated that one carbamoyl group is 6-*O*-linked, while the other is presumed to be either 3-*O*- or 4-*O*-linked. Furthermore, the more polar NodNGR_A Nod factors differ from the NodNGR_B factors by substitutions on the 2-*O*-MeFuc residue. The NodNGR_A compounds were 3-sulfated on this sugar, whereas the NodNGR_B factors were either 4-*O*-acetylated or non-substituted. We have previously shown that acetylation or sulfation of the fucosyl residue at least partially determines the host-specific biological activity of the NGR234 Nod factors [1].

Nod factors isolated from narrow host range *Rhizobium* have been shown to be *N*-acylated chitomers which are structurally modified by the presence of appropriate rhizobial host-specificity *nod* genes [2,9]. However, the range of modifications is quite small and the diversity of Nod factors secreted by narrow host range *Rhizobium* strains is relatively few [2,9]. By contrast, broad host-range *Rhizobium* sp. NGR234 produces a large number of Nod factors, and modifications to the core *N*-acyl chitomer structure included *O*-carbamoylation and *N*-methylation of the acylated nonreducing sugar, and 6-*O*-substitution of the reducing *N*-acetylglucosamine with either 4-*O*-acetylated or 3-sulfated 2-*O*-methylfucose. Recently, Nod factor carbamoylation and *N*-methylation has been attributed to the presence of *nodU* and *nodS* genes, respectively [28], and the α -(1 \rightarrow 6)-L-fucosyltransferase gene to *nodZ* [29]. Structural assignments presented here suggest the probable presence of other enzymes involved Nod factor biosynthesis in *Rhizobium* sp. NGR234, notably α -L-fucosyl-specific 2-*O*-methyltransferase, 3-*O*-sulfo-transferase, and 4-*O*-acetyltransferase activities.

Acknowledgements

We thank J. Dénarié and R.W Carlson for helpful discussion. M. O'Neil helped with ESMS. N.P.J.P was the recipient of an EMBO short term Fellowship and also acknowledges the DOE grant (DE-FG09-87ER13810) to the Complex Carbohydrate Research Center, Athens, GA.

References

- [1] N.P.J. Price, B. Relic, F. Talmont, A. Lewin, D. Promé, S.G. Pueppke, F. Maillet, J. Dénarié, J.-C. Promé, and W.J. Broughton, *Mol. Microbiol.*, 6 (1992) 3575–3584.
- [2] R.W. Carlson, N.P.J. Price, and G. Stacey, *Mol. Plant-Microbe Interact.*, 7 (1995) 684–695.
- [3] J.L. Firmin, K.E. Wilson, L. Rossen, and A.W.B. Johnson, *Nature*, 324 (1986) 90–94.
- [4] P. Lerouge, P. Roche, C. Faucher, F. Maillet, G. Truchet, J.-C. Promé, and J. Dénarié, *Nature*, 344 (1990) 781–784.
- [5] M. Schultze, B. Quiclet-Sire, E. Kondorosi, H. Virelizier, J.N. Glushka, G. Endre, S.D. Gèro, and A. Kondorosi, *Proc. Natl. Acad. Sci. USA*, 89 (1992) 192–196.
- [6] H.P. Spaink, D.M. Sheeley, A.A.N. van Brussel, J. Glushka, W.S. York, T. Tak, O. Geiger, E.P. Kennedy, V.N. Reinhold, and B.J.J. Lugtenberg, *Nature*, 354 (1991) 125–130.
- [7] G. Truchet, P. Roche, P. Lerouge, J. Vasse, S. Camut, F. De Billy, J.-C. Promé, and J. Dénarié, *Nature*, 351 (1991) 670–673.
- [8] P. Roche, F. Debellé, F. Maillet, P. Lerouge, C. Faucher, G. Truchet, J. Dénarié, and J.-C. Promé, *Cell*, 67 (1991) 1131–1143.
- [9] P. Lerouge, *Glycobiology*, 4 (1994) 127–124.
- [10] B. Relic, X. Perret, M.T. Estrada-Garcia, J. Kopicinska, W. Golinowski, H.B. Krishnan, S.G. Pueppke, and W.J. Broughton, *Mol. Microbiol.*, 13 (1994) 171–178.
- [11] J.P. Kamerling, G.J. Gerwig, J.F.G. Vliegthart, and J.R. Clamp, *Biochem. J.*, 151 (1975) 491–495.
- [12] G.J. Gerwig, J.P. Kamerling, and J.F.G. Vliegthart, *Carbohydr. Res.*, 77 (1979) 1–7.
- [13] J.-C. Promé, H. Aurelle, F. Couderc, and A. Savagnac, *Rapid Commun. Mass Spectrom.*, 1 (1987) 50–52.
- [14] K. Yamamoto, A. Shibahara, T. Nakayama, and G. Kajimoto, *Chem. Phys. Lipids*, 60 (1991) 39–50.
- [15] I. Yruela, A. Barba, and J.O. Grimalt, *J. Chromatogr. Sci.*, 28 (1990) 421–427.
- [16] J.P. Parente, P. Cardon, Y. Leroy, J. Montreuil, B. Fournet, and G. Ricard, *Carbohydr. Res.*, 141 (1985) 41–46.
- [17] B. Domon and C.E. Costello, *Glycoconjugate J.*, 5 (1988) 397–409.
- [18] J.F.G. Vliegthart, L. Dorland, and H. van Halbeek, *Adv. Carbohydr. Chem. Biochem.*, 41 (1983) 209–373.
- [19] J.-C. Michalski, J.-M. Wieruszkeski, C. Alonso, P. Cache, J. Montreuil, and G. Strecker, *Eur. J. Biochem.*, 201 (1991) 439–458.
- [20] W. Chai, E.F. Hounsell, G.C. Cashmore, J.R. Rosankiewicz, C.J. Bauer, J. Feeney, T. Feizi, and A.M. Lawson, *Eur. J. Biochem.*, 207 (1992) 973–980.
- [21] G. Lamblin, H. Rahmoune, J.-M. Wieruszkeski, M. Lhermitte, G. Strecker, and P. Roussel, *Biochem. J.*, 275 (1991) 199–206.
- [22] T. Usai, Y. Hayashi, K. Sakia, and Y. Ishido, *Biochim. Biophys. Acta*, 923 (1987) 302–309.
- [23] Y. Kawakami, K. Yamasaki, and S.J. Nakamura, *J. Antibiot.*, 34 (1981) 921–922.
- [24] G. Weisshaar, J. Hiyama, and G.C. Renwick, *Glycobiology*, 1 (1991) 393–404.
- [25] H. Naganawa, K. Muraoka, T. Takita, and H. Umezawa, *J. Antibiotics*, 30 (1977) 388–396.
- [26] S. Kusumoto, Y. Kambayashi, S. Imaoka, K. Shima, and T. Shiba, *J. Antibiot.*, 35 (1982) 92531.
- [27] M. Gilleron, A. Venisse, M. Riviére, P. Servin, and G. Puzo, *Eur. J. Biochem.*, 193 (1990) 449–457.
- [28] S. Jabbouri, R. Fellay, F. Talmont, P. Kamalaprija, U. Burger, J.-C. Prome, and W.J. Broughton, *J. Biol. Chem.*, 270 (1995) 22968–22973.
- [29] G. Stacey, S. Luka, J. Sanjuan, Z. Banfalvi, A.J. Nieuwkoop, J.Y. Chun, L.S. Forsberg, and R.W. Carlson, *J. Bacteriol.*, 176 (1994) 620–633.